Tmem27: A cleaved and shed plasma membrane protein that stimulates pancreatic β cell proliferation

Pinar Akpinar, Satoru Kuwajima, Jan Krützfeldt, and Markus Stoffel*

Laboratory of Metabolic Diseases, The Rockefeller University, 1230 York Avenue, New York, New York 10021
*Correspondence: stoffel@mail.rockefeller.edu

Summary

The signals and molecular mechanisms that regulate the replication of terminally differentiated β cells are unknown. Here, we report the identification and characterization of transmembrane protein 27 (Tmem27, collectrin) in pancreatic β cells. Expression of Tmem27 is reduced in *Tcf1*$^{-/-}$ mice and is increased in islets of mouse models with hypertrophy of the endocrine pancreas. Tmem27 forms dimers and its extracellular domain is glycosylated, cleaved and shed from the plasma membrane of β cells. This cleavage process is β cell specific and does not occur in other cell types. Overexpression of full-length Tmem27, but not the truncated or soluble protein, leads to increased thymidine incorporation, whereas silencing of Tmem27 using RNAi results in a reduction of cell replication. Furthermore, transgenic mice with increased expression of Tmem27 in pancreatic β cells exhibit increased β cell mass. Our results identify a pancreatic β cell transmembrane protein that regulates cell growth of pancreatic islets.

Introduction

Beta cell hyperplasia is an important adaptive mechanism to maintain normoglycemia during physiological growth and in obesity. Increasing evidence suggests that β cell mass is dynamic and that increased demands on insulin secretion in insulin resistance and pregnancy can lead to rapid and marked changes in β cell mass (Bruning et al., 1997; Accili, 2001; Bonner-Weir, 2000a; Sorenson and Brelje, 1997). The mass of β cells is governed by the balance of β cell growth (replication) and by β cell death (apoptosis) (Lingohr et al., 2002; Butler et al., 2003; Flier et al., 2001; Bonner-Weir, 2000b). However, the identity of the factors that control β cell mass remain elusive. Understanding how β cell mass is regulated is important to design rational approaches to prevent pancreatic β cell loss in insulin-resistant states and to expand β cells for transplantation in type 1 diabetes.

During development, β cells are generated from a population of pancreatic progenitor cells (Edlund, 2002; Wilson et al., 2003). The β cells that differentiate from progenitor cells are postmitotic, and direct lineage tracing studies indicate that a population of progenitor cells persists throughout embryogenesis to allow the differentiation of new β cells (Gu et al., 2002; Gradwohl et al., 2000; Dor et al., 2004). In the neonatal period new β cells are formed by replication of differentiated β cells, which results in a massive increase in β cell mass (Finegood et al., 1995; Svenstrup et al., 2002). In adulthood there is little increase in the β cell number except in conditions of increased demand. During pregnancy a marked hyperplasia of β cells is observed both in rodents and man. This is due to increased mitotic activity of β cells exposed to placental lactogen (PL), prolactin (PRL), and growth hormone (GH) (Svenstrup et al., 2002; Parsons et al., 1995; Scaglia et al., 1995). The growth stimulatory signals in pathological insulin resistant states are less well understood.

Several mouse models of insulin resistance and diabetes, such as the *ob*/*ob* and *db*/*db* mice or mutant mice created by inactivation of the gene for insulin receptor substrate-1 (Irs-1) or double heterozygous (DH) knockout of the insulin receptor and Irs-1, exhibit marked islet hyperplasia (Bock et al., 2003; Tomita et al., 1992; Kulkarni et al. 2002, 2004; Kahn, 2003). In contrast, loss of Irs-2 function leads to a dramatic reduction of β cells and diabetes (Withers et al., 1998). Glucose itself is known to stimulate β cell replication (Topp et al., 2004), however, many of the above mouse models increase their total islet mass before the onset of detectable hyperglycemia. Furthermore, in most cases the hyperplastic response bears no relationship to the level of hyperglycemia, suggesting that factors independent of glucose are likely to contribute to the islet growth.

Endocrine pancreatic growth during development depends on multiple transcription factors that display highly specific temporal and spatial expression patterns that control mechanisms for cell differentiation (Edlund, 2002). During early pancreatic development, cell fate decisions and differentiation of endocrine progenitor cells into hormone-producing islet cells are tightly regulated by the sequential expression of specific transcription factors (Wilson et al., 2003). The expression of these factors is also important for maintaining normal pancreatic β cell function in adult life. For instance, mutations in several transcription factors lead to a subtype of type 2 diabetes called maturity-onset diabetes of the young (MODY), which are characterized by autosomal dominant inheritance, an early age of disease onset, and development of marked hyperglycemia with a progressive impairment in insulin secretion (Shih and Stoffel, 2002). The most frequent form of MODY is caused by mutations in the gene encoding hepatocyte nuclear factor-1α (HNF-1α, TCF1). Mutant mice with loss of Tcf1 function as well as transgenic mice expressing a naturally occurring dominant-negative form of human *TCF1*(P291fsinsC) in pancreatic β cells develop progressive hyperglycemia due to impaired glucose-stimulated insulin secretion (Hagenfeldt-Johansson et al., 2001; Yamagata et al., 2002). Importantly, these mice exhibit a progressive reduction in β cell number, proliferation rate, and pancreatic insulin content.

These data indicate that Tcf-1 target genes are also required for maintenance of normal β cell mass.

In this study we sought to identify target genes of Tcf-1 that may be responsible of mediating β cell growth by comparing gene expression profiles of *Tcf-1*$^{-/-}$ and wild-type littermates in isolated pancreatic islets. This analysis led to the identification of a transcript encoding transmembrane protein-27 (Tmem27) that is markedly reduced in pancreatic islets of *Tcf-1*$^{-/-}$, mice compared to controls. Tmem27 was originally described as a kidney-specific gene that is upregulated in an injury-induced renal hypertrophy model and termed collectrin (Zhang et al., 2001). In this study, we carried out a comprehensive biochemical and functional analysis that demonstrates that Tmem27 is a stimulator of β cell replication in vitro and in vivo.

Results

Tmem27 expression is regulated by Tcf1

In an attempt to identify mitogenic factors in pancreatic β cells, we compared gene expression in isolated pancreatic islets of *Tcf1*$^{-/-}$ and wild-type littermates using Affymetrix™ oligonucleotide expression arrays (see Supplemental Experimental Procedures in the Supplemental Data available with this article online). Two replicates were independently analyzed (deposited at GEO-NCBI under accession number GSE3544). This analysis identified a gene encoding a transmembrane-spanning protein (Tmem27) that showed a 16-fold decrease in expression levels of *Tcf1*$^{-/-}$ mice compared to controls. This result was confirmed by RT-PCR in an independent group of animals (Figure 1A). To study whether Tcf1 is a direct activator of Tmem27 transcription, we analyzed the Tmem27 promoter and identified two putative Tcf1 binding sites in its regulatory region that were conserved between human and mouse (Figure 1B). We cloned an 815 bp promoter region upstream of a luciferase reporter gene and coexpressed it with a Tcf1 expression vector. Transient cotransfection of Tcf1 and Tmem27 promoter led to a >5-fold activation of luciferase activity (Figure 1C). When each Tcf1 site in the Tmem27 promoter was selectively mutated, transcriptional activation was reduced 70%–80% (Figure 1C). To demonstrate binding of Tcf1 to these sites in vitro we carried out electrophoretic gel mobility shift assays (EMSA) using double stranded ^{32}P-labeled oligonucleotides containing the respective Tcf binding sites and MIN6 cell extracts. Figure 1D shows that the probe shifted upon addition of nuclear extracts and that the binding could be competed by adding increasing amounts of a known binding site of the farnesoid X receptor promoter (Fxr) (Shih et al., 2001). The specificity of protein binding to these sites was also determined by further shifting the DNA-Tcf1 complex using a specific anti-Tcf1 antiserum (Figure 1D). We also investigated if Tcf1 directly increases the expression of Tmem27 by performing chromatin immunoprecipitation assays (ChIP). Tcf1 bound to the binding sites in the Tmem27 promoter of MIN6 cells and pancreatic islets but not in primary hepatocytes where Tmem27 is not expressed (Figure 1E). These data confirm the functionality of the Tcf1 binding sites in vivo and demonstrate that Tcf1 is required for expression of Tmem27 in pancreatic β cells.

TMEM27 is regulated during pancreas development

Expression of Tmem27 was studied during mouse pancreatic development by immunohistochemical staining. In newborn and adult pancreas, Tmem27 expression is restricted to β cells of the islet (Figure 2, data not shown). During development of the pancreas, Tmem27 is expressed at the earliest time when hormone positive (mainly glucagon-positive cells) are apparent. At embryonic days E10.5 and E12.5 Tmem27 expression is localized in cells that express glucagon and insulin. During the peak period of endocrine cell expansion, from embryonic day 13.5 to 18.5, Tmem27 mainly colocalizes with glucagon until right before birth at E18.5 when it is also detected in insulin positive cells (Figure 2).

Tmem27 is an N-linked glycoprotein and forms dimers in vivo

Tmem27 contains two predicted N-glycosylation sites at amino acid residues 76 and 93, respectively. MIN6 cells were treated with tunicamycin, an inhibitor of N-glycosylation (Waechter and Lennarz, 1976). Cells were incubated in the presence of increasing concentrations of tunicamycin and protein extracts were prepared and analyzed by SDS-PAGE and immunoblotting. Two bands with increased electrophoretic mobility appeared upon treatment with tunicamycin, whereas the high molecular weight protein disappeared (Figure 3A). This result was confirmed with an in vitro assay using N-glycanase, an enzyme that releases intact N-linked glycans (data not shown). These data suggest that Tmem27 is an N-linked glycoprotein.

We also carried out chemical cross-linking experiments to test if Tmem27 protein exists as a multimer. MIN6 cell extracts were incubated in the presence of two different cross-linking reagents: BMH (bismaleimidohexane), a membrane-permeable, noncleavable compound and DTBP (dimethyl 3, 3′-dithiobispropionimidate), a membrane permeable, cleavable compound. Following these treatments, an SDS-PAGE analysis was performed under reducing and nonreducing conditions (Partis et al., 1983; Geisler et al. 1992). Nonreducing western blots revealed a band of exactly twice the molecular weight than under reducing conditions. Cell extracts treated with BMH showed the dimer protein in both reducing and nonreducing blots. In contrast, the protein dimers disappeared under reducing conditions in the presence of DTBP (Figure 3B). The results were similar in MIN6 cells that endogenously express Tmem27 and in N2A cells that were transiently transfected with Tmem27 expression vector (data not shown).

Tmem27 is cleaved and shed from pancreatic β cells

Tmem27 has previously been predicted to be a transmembrane protein with an N-terminal extracellular domain (Zhang et al., 2001). We generated two antibodies (α-Tmem27N and α-Tmem27C) that recognize peptides from extra- and intracellular domains of the protein, respectively (Figure 4A). In Western blotting experiments anti-Tmem27C detected two bands in whole-cell lysates of MIN6 cells (Figure 4B). The higher molecular weight band corresponded to the predicted molecular weight of the glycosylated full-length protein. The lower band (~25 kDa) was also specific since it could be detected by Western blotting in cell lysates following transfection with a vector (p-Tmem27.V5) expressing a C-terminal V5-Tag fusion protein and an anti-V5 antibody (Figure 4B). We hypothesized that Tmem27 might be cleaved and possibly shed, with the lower molecular weight band representing the C-terminal transmembrane spanning part of Tmem27. We therefore analyzed supernatants from different cell lines (including neuronal N2A cells,

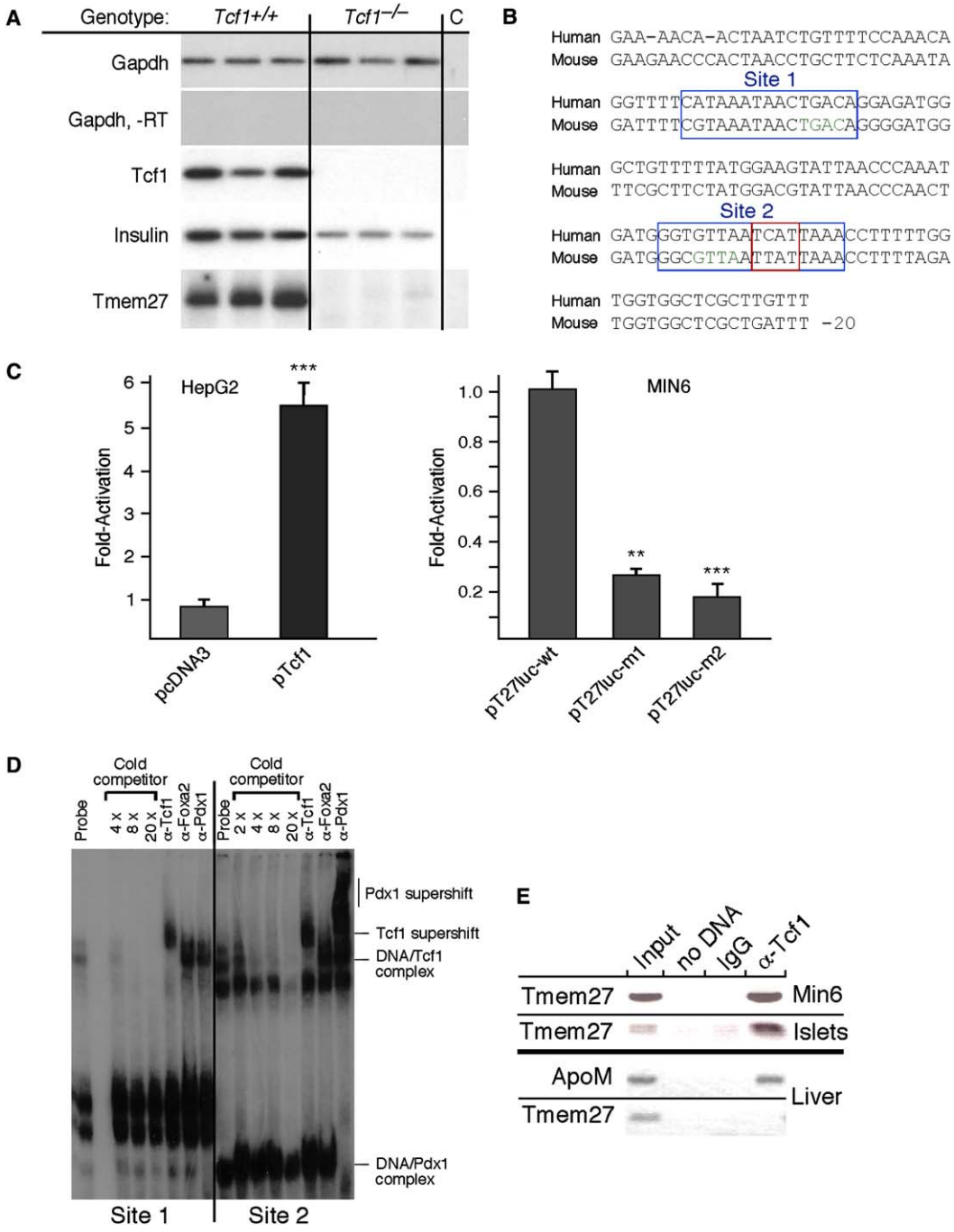

Figure 1. Tmem27 expression is regulated by Tcf1

A) Tmem27 expression is decreased in the islets of *Tcf1*$^{-/-}$ mice compared to wild-type littermate controls. Expression levels were measured with RT-PCR, GAPDH was used as a control. C, no DNA added; −RT, no reverse transcriptase added to reaction.

B) Promoter analysis predicted two conserved Tcf binding sites in the upstream regulatory regions of human and mouse (bottom) *Tmem27* genes, at −60 and −117 base pairs relative to the transcriptional start site. Human (top) and mouse (bottom) promoter sequences are aligned and Tcf binding sites are boxed in blue. A second site (red box) denotes a putative Pdx-1 binding site. Highlighted sequences (green) indicate positions of the mutated Tcf binding sites.

C) Transcriptional activation assays in HepG2 cells that were transfected with pcDNA3 or pTcf1, pCMV-β-glactosidase, and the luciferase reporter gene using a 815 bp Tmem27 mouse promoter (left panel). Tcf binding sites were mutated individually in the promoter sequence of the reporter vector and MIN6 cells were transfected with vectors pT27luc-wt, pT27luc-m1 or p27luc-m2. Luciferase activity was normalized to β-galactosidase activity (right panel). Each value represents the mean of eight independent experiments. *$p < 0.05$, **$p < 0.01$, ***$p < 0.001$.

D) EMSA analysis using oligonucleotides for Tcf binding sites 1 and 2 and whole-cell extracts of MIN6 cells. Competitor represents unlabeled double-stranded oligonucleotides at increasing concentrations containing Tcf1 binding site of Fxr-1 promoter (Shih et al., 2001). The signal of the free probe at the bottom of the gel was cut off.

E) Chromatin immunoprecipitation assays in pancreatic islets and MIN6 cells demonstrate an in vivo interaction of Tcf1 with the promoter of Tmem27. A 150 bp region spanning binding sites 1 and 2 was amplified with PCR. This interaction could not be found in primary hepatocytes, which do not express Tmem27. ChIP for Tcf1 was validated in primary hepatocytes by amplification of a region in apolipoprotein M (apoM) promoter that spans the Tcf1 binding site (Richter et al., 2003).

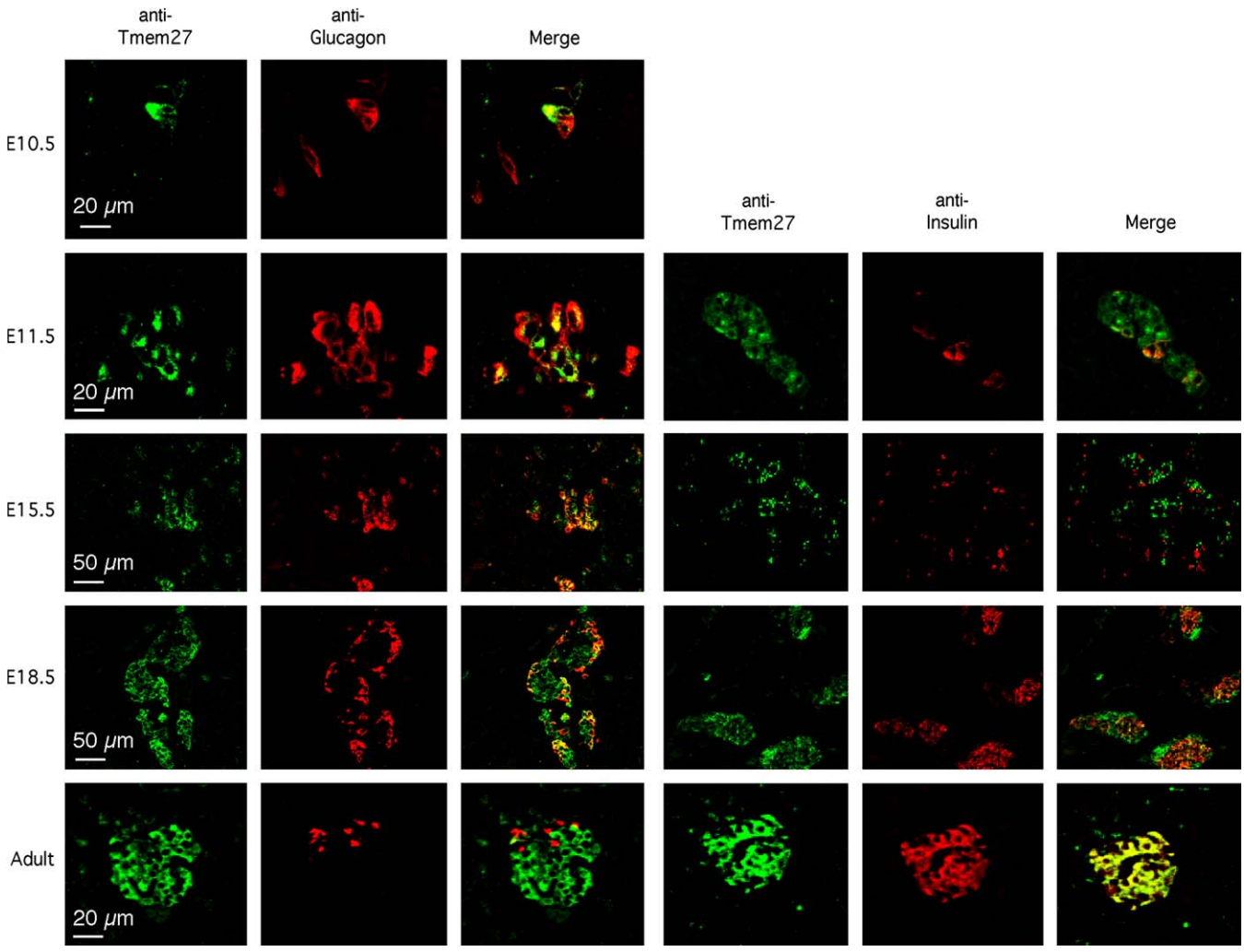

Figure 2. Tmem27 is expressed in the developing mouse pancreas

Immunofluorescence of paraffin embedded pancreatic tissue from denoted time points in the mouse development with anti-Tmem27C, anti-Insulin and anti-Glucagon antibodies. Developmental stages are indicated as embryonic (E) days.

HepG2 cells, HEK293, and M-1 cells that were derived from collecting ducts of the kidney and which exhibit endogenous expression of Tmem27). Cells were cultured for 48 hr in reduced-serum medium and Tmem27 immunoreactivity in the supernatant was assayed by Western blotting using anti-Tmem27N. We detected a band corresponding to a ~25 kDa protein in clonal β cell lines MIN6 and INS1E (Figure 4C, data not shown). Interestingly, this protein can only be detected in the supernatant but not in whole-cell lysates, indicating that cleavage occurs at the outer plasma membrane. This cleaved form of Tmem27 could also be detected in media incubated with isolated mouse pancreatic islets (Figure 4D). Treatment of supernatants with N-Glycanase led to the disappearance of the ~25 kDa protein and the emergence of a band at ~12 kDa, the expected molecular weight of the unglycosylated N-terminal domain of Tmem27 (Figure 4E). Interestingly, in spite of robust expression of full-length protein in cell-lysates, we failed to detect this band in Western blot analysis in the culture medium of non-β cell lines that were transiently transfected with a Tmem27 expression vector (pTmem27). In contrast, overexpression of Tmem27 in MIN6 and INS1E cells led to increased amounts of soluble protein in their culture media (Figure 4C, data not shown). We also showed that siRNA-mediated reduction in Tmem27 protein levels correlated with decreased levels of the soluble form of Tmem27 in MIN6 cell supernatants (Figure 4F). Lastly, in order to irrefutably prove that N-terminal portion of Tmem27 is cleaved and shed from β cells an expression vector (pTmem27-HA) was generated in which a nine amino acid HA-epitope tag was inserted downstream of amino acid residues 39 of the Tmem27 protein (Figure 4A). MIN6 cells transfected with this vector released a protein in the supernatants that could be detected with an anti-HA antibody and had a similar size as untagged Tmem27. This protein was not detected in control cells or cells expressing the untagged protein (Figure 4G). Together, these data demonstrate that Tmem27 is a pancreatic β cell-specific, cleaved and shed transmembrane protein.

Tmem27 is a constitutively shed plasma membrane protein

To localize Tmem27 in pancreatic β cells, we performed immunofluorescence studies using anti-Tmem27N and –C antibodies. MIN6 or dispersed pancreatic islets were grown on slides, fixed

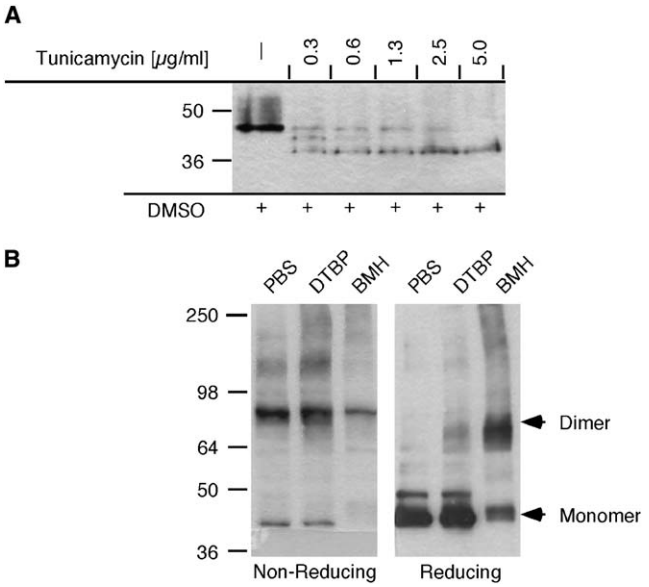

Figure 3. Tmem27 is an N-glycosylated protein and forms dimers

A) MIN6 cells were incubated with increasing amounts of tunicamycin, which inhibits glycosylation at asparagine residues. Addition of DMSO alone to the cells had no effect.

B) MIN6 cell lysates were incubated with either PBS, or cross-linking reagents dimethyl 3, 3′-dithiobispropionimidate (DTBP) and bismaleimidohexane (BMH). SDS-PAGE under nonreducing conditions and immunoblotting using anti-Tmem27C antibodies showed a band twice the molecular weight of full-length Tmem27. Under reducing conditions, only the monomer was detected in PBS and DTBP-treated cell lysates. In contrast, the dimer persisted in BMH-treated samples as BMH cross-linking could not be reversed.

and permeabilized and treated with primary antibodies raised against insulin and synaptophysin (*Syn*), specific markers for insulin-containing dense-core granules and synaptic-like microvesicles, respectively (Wiedenmann et al., 1988). Neither insulin nor synaptophysin colocalized with Tmem27, demonstrating that Tmem27 is not a constituent of these organelles (Figure 5A). Specific staining of Tmem27 was detected in the perinuclear compartment and on the plasma membrane. Plasma membrane staining of Tmem27 colocalized with membrane immunoreactivity of Glut2, further supporting that Tmem27 is a surface-membrane protein. We also studied Tmem27 by electron microscopy and observed nanogold particles associated with the plasma membrane in proximity to vesicle /membrane fusion events (Figures 5B and 5C). To further investigate the release of the cleaved form of Tmem27 we stimulated isolated pancreatic islets cells with low (2.8 mM) and high (11.1 mM) glucose concentrations. Whereas insulin secretion increased when stimulated with glucose we did not measure a change in Tmem27 concentrations in the supernatant of these cells (Figure 5D). Lastly, we performed pulse-chase experiments using ^{35}S-methionine to determine the kinetics of uncleaved and soluble Tmem27 proteins. [^{35}S]methionine incorporation in Tmem27 was calculated from band densities on scanned autoradiography films. Relative immunoprecipitated radioactivity on the gels showed that [^{35}S]methionine was incorporated in Tmem27 protein for up to 3 hr after the start of the chase period. This time point is denoted as 100% incorporation (Figure 5E). The half-life of Tmem27 from linear regression analysis of the data points was determined to be ~27 hr. [^{35}S]-labeled, soluble Tmem27 was immunoprecipitated from MIN6 supernatants and quantitated by scintillation counting after PAGE. Relative radioactivity present in the bands over a period of 24 hr revealed that the amount of cleaved Tmem27 in the supernatant of MIN6 cells increased linearly and by approximately 10% every hour. These data show that soluble Tmem27 is shed into the supernatant in a constitutive manner.

Increased expression of TMEM27 in mouse models with islet hypertrophy and enhanced β cell replication in vitro

We measured expression of Tmem27 in hypertrophied islets of *ob/ob*, *db/db* and *aP2-Srebp-1c* transgenic mice (Shimomura et al., 1998). Pancreatic islets from 6- to 8-week-old mice were isolated and gene expression levels were compared to their wild-type littermates. Using real-time PCR we found a 1.7, 1.7, and 2.7-fold increase in Tmem27 levels of *ob/ob*, *db/db*, and *aP2-Srebp-1c* islets, respectively, compared to controls (Figure 6A). In addition, islets isolated from these mice exhibited an increase in secretion of cleaved Tmem27 into the medium compared to size-matched islets of wild-type littermates (Figure 6B, data not shown). To study if Tmem27 stimulates pancreatic β cell replication, we examined the effect of Tmem27 expression on the proliferation of MIN6 cells. Cells were electroporated with either siRNAs targeting Tmem27 or plasmid pTmem27. Cell replication was assessed by cell counting and measuring incorporation of [^{3}H]thymidine 48 hr after electroporation (Figures 6C and 6D). MIN6 cells that were transfected with pTmem27 exhibited ~5-fold overexpression compared to pcDNA3-transfected cells and showed ~2-fold increase in [^{3}H]thymidine incorporation and increased cell density 48 hr after plating. In contrast, MIN6 cells that had reduced expression of protein following siRNA treatment showed lower [^{3}H]thymidine incorporation and cell density (Figures 6C and 6D). Furthermore, we did not observe any changes in apoptosis in cells with increased or reduced expression of Tmem27 (data not shown), suggesting Tmem27 does not affect cell death. To further elucidate if the full-length, truncated, or soluble form of Tmem27 stimulated β cell replication in vitro we generated a Tmem27 mutant (pTmem27-V5.del.) in which amino-acid residues 17-129 were deleted. Transfection of pTmem27-V5.del. in MIN6 cells led to the expression of a truncated protein of ~30 kDa (Figure 6E). [^{3}H]thymidine incorporation assays demonstrated that expression of the full-length Tmem27 increased replication not only in MIN6 cells but also in HepG2 and HEK293 cells. In contrast, overexpression of the truncated Tmem27 form showed no effect (Figure 6F). Since non-β cell lines do not release the soluble Tmem27 form these data demonstrate that the full-length form of Tmem27 is responsible for the proliferation response. Independent evidence that the soluble form has no effect on cell replication was obtained from coculture and conditioned medium experiments in which cells were cultured with increasing concentrations of soluble Tmem27 (data not shown). Together, these results demonstrate that the full-length form of Tmem27 stimulates cell proliferation in MIN6 and other cell types.

Trangenic mice overexpressing Tmem27 in pancreatic islets exhibit islet hypertrophy

We generated two independent pancreatic β cell-specific transgenic lines following pronuclear microinjection of a vector construct in which the murine Tmem27 cDNA is under the control of the rat insulin promoter. RT-PCR and immunoblot analysis

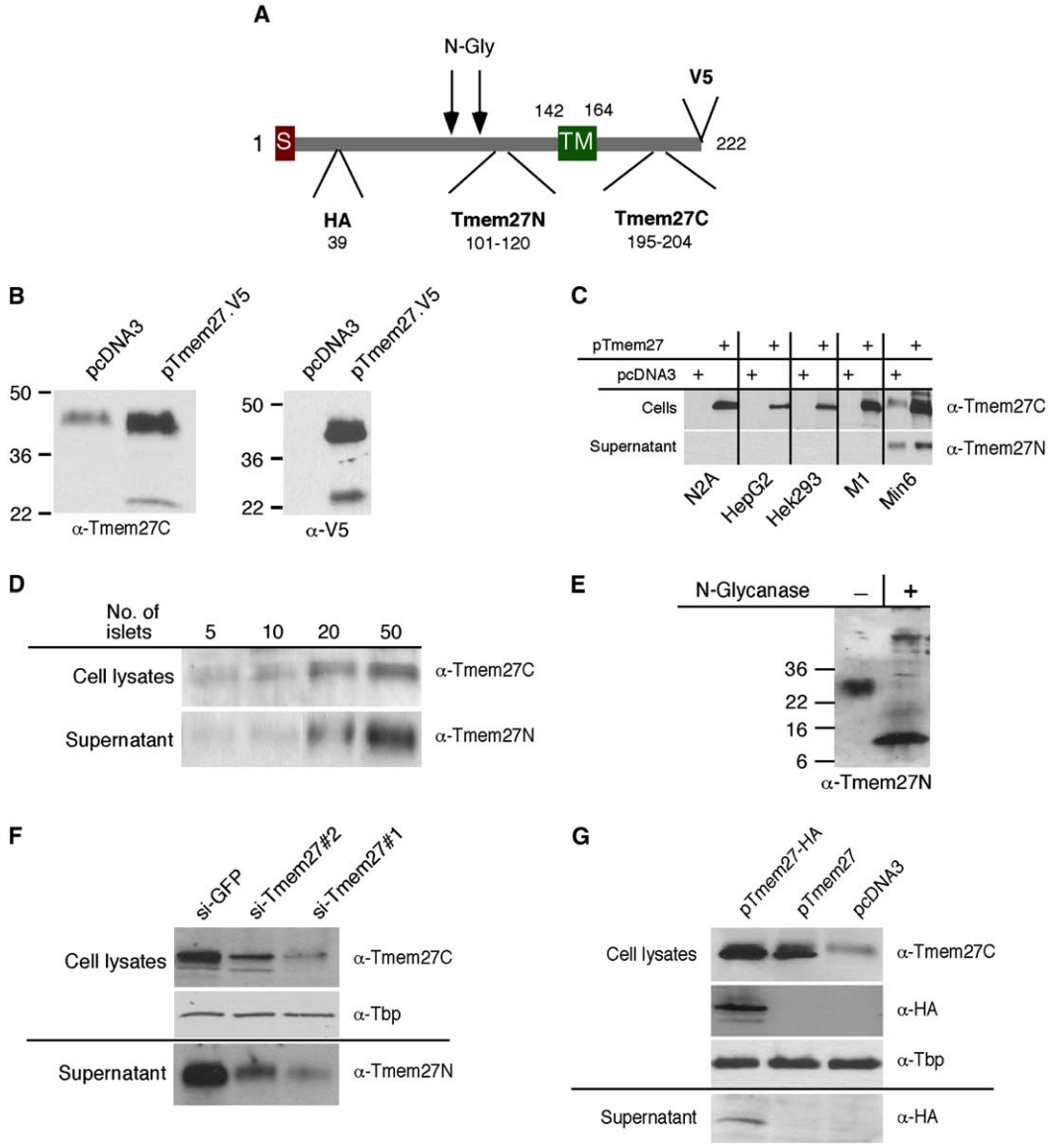

Figure 4. TMEM27 is cleaved and released from β cells of the islet

A) Schematic drawing of TMEM protein domains, including regions against which antipeptide antibodies were raised and epitopes were inserted. Numbers denote positions of amino acid residues. S, signal peptide sequence; TM, transmembrane domain; N-Gly, N-glycosylation sites; HA, position of HA-epitope insertion; V5, position of V5-epitope insertion; Tmem27N and Tmem27C indicate positions of sequences used for antipeptide antibody production.

B) Anti-Tmem27C antibody in Western blots of MIN6 cells detected two bands for Tmem27 (left panel). The 25 kDa band became more abundant in cells that were transfected with pTmem27.V5.

Immunoblots of cell lysates from above were probed with α-V5 antibody (right panel). The antibody against the V5-epitope also detected both bands in pTmem27.V5-transfected cells but not in pcDNA3-transfected cells.

C) Denoted cell lines were transfected with pcDNA3 or pTmem27 and full-length protein was detected with anti-Tmem27C in Western blots of cell lysates. Soluble protein was detected with anti-Tmem27N only in the supernatant of MIN6 cells. Increased expression of full-length protein led to increased amounts of soluble protein solely in the MIN6 cells. Supernatants were collected after 48 hr and normalized to protein content of cell lysates.

D) Mouse pancreatic islets were isolated and incubated for 72 hr. Supernatants were collected and islets were transferred in lysis buffer. Full-length protein was detected with anti-Tmem27C in Western blots of lysates and soluble protein was detected with anti- anti-Tmem27N in Western blots loaded with equal volumes of the supernatant.

E) Supernatant from MIN6 cells was incubated with N-glycanase. The molecular weight shift in the Western blot indicates that the enzyme removed sugar moieties from soluble Tmem27. Soluble protein was detected with anti-Tmem27N antibody.

F) MIN6 cells were electroporated with siRNAs targeting GFP or Tmem27. In the cells that were electroporated with si-Tmem27#1 and #2, reduction in the levels of Tmem27 protein was detected with anti-Tmem27C 48 hr after electroporation. SDS-PAGE was run with supernatants from the same cells and reductions in the levels of soluble proteins were detected with anti-Tmem27N. Supernatants were collected after 48 hr and normalized to protein content of cell lysates.

G) MIN6 cells were electroporated with pcDNA3, pTmem27 or pTmem27-HA. Overexpression of Tmem27 was detected by Western blotting of cell lysates with anti-Tmem27C antibodies. Supernatants from the same cells were collected after 48 hr and subjected to Western blotting with anti-HA epitope antibody.

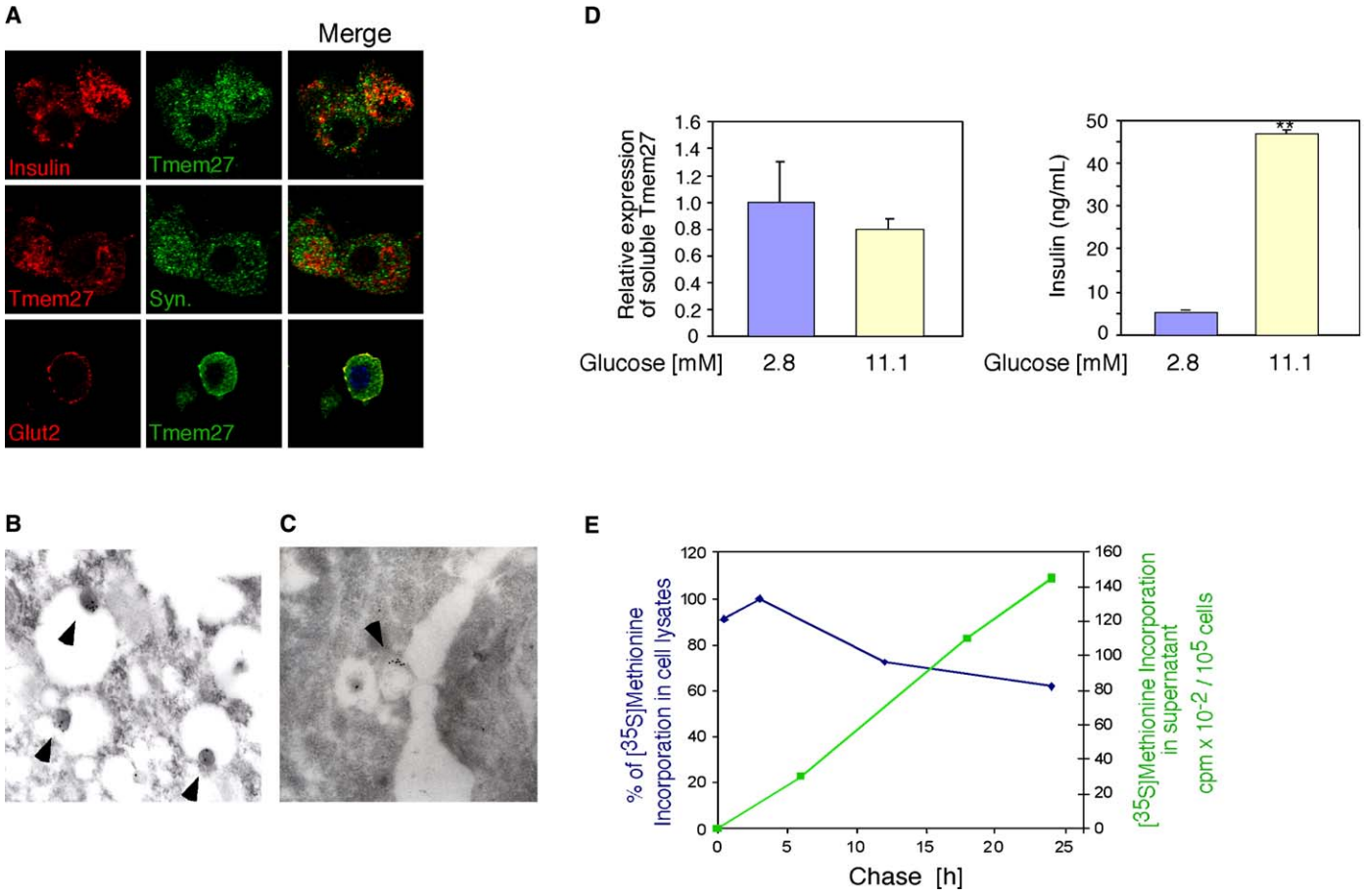

Figure 5. Tmem27 is located in secretory vesicles and on plasma membranes of pancreatic β cells

A) Isolated mouse islets were dispersed and stained with anti-Tmem27C and anti-Insulin, anti-Synaptophysin, or anti-Glut-2 antibodies.

B) Electron microscopy performed on MIN6 cells with anti-Tmem27C antibodies localized Tmem27 in small secretory vesicles (arrows). IgG conjugated to 10 nm gold particles was used for detection of the antibody.

C) Using the same method as in (**B**), vesicles that contain Tmem27 were detected during fusion events with the plasma membrane (arrow).

D) An equal number of size-matched mouse islets were incubated in either 2.8 mM or 11.1 mM glucose. Supernatants were collected after 72 hr and soluble Tmem27 levels were quantified and normalized to protein content of islet lysates. Secreted insulin levels were measured after 6 hr incubation in the same supernatant. $^{**}p < 0.0002$.

E) [^{35}S]Methionine incorporation into Tmem27 was measured in MIN6 cells during a pulse-chase experiment over 24 hr.

showed that Tmem27 expression in both lines was ~4-fold increased in pancreatic islets compared to wild-type littermates (Figure 7A). We studied the islet mass at ages 10 and 20 weeks in transgenic animals by pancreatic islet morphometry. Transgenic mice exhibited normal islet morphology (based on immunohistochemistry using insulin/glucagon costaining) but had an approximately 1.5- and 2-fold increase in islet mass at 10 and 20 weeks, respectively, compared to wild-type littermates (Figures 7B and 7C, data not shown). No difference was found in the mass of non-β cells (α-, γ-, and δ cells) (Figure 7D). The increase in β cell mass was further validated by measuring the total insulin content of transgenic and wild-type mice. The total insulin content was also increased in transgenic mice overexpressing Tmem27 (Figure 7E). To rule out that increased insulin resistance was responsible for the observed increase in β cells mass we performed insulin-tolerance tests (ITT). No difference in glucose clearance following a bolus insulin injection was observed (data not shown). Furthermore, no significant difference in body weight, fasting insulin levels, plasma leptin concentrations and adiponectin levels were measured in transgenic mice compared to control littermates (data not shown). These data show that insulin resistance is not responsible for the increased β cell mass observed in the transgenic animals. Increased β cell replication may lead to decreased glucose responsiveness due to dedifferentiation. Therefore, we performed glucose tolerance tests and studied insulin secretion from islets that were isolated from either wild-type or transgenic animals. Transgenic mice exhibited normal glucose tolerance (data not shown) and we observed a robust ~13-fold increase in insulin secretion of islets isolated from transgenic mice in response to glucose stimulation, comparable to wild-type controls (Figure 7F). Together, these data demonstrate that Tmem27 stimulates islet growth in vivo and that increased expression of Tmem27 does not impair regulated insulin secretion and glucose sensing.

Discussion

In this study we used a genomic approach to identify genes that may contribute to maintenance of islet mass during adult life and enhancing islet growth when the demand for insulin secretion increases. We found that Tmem27 exhibits markedly reduced expression in diabetic *Tcf1*$^{-/-}$ animals with decreased islet mass

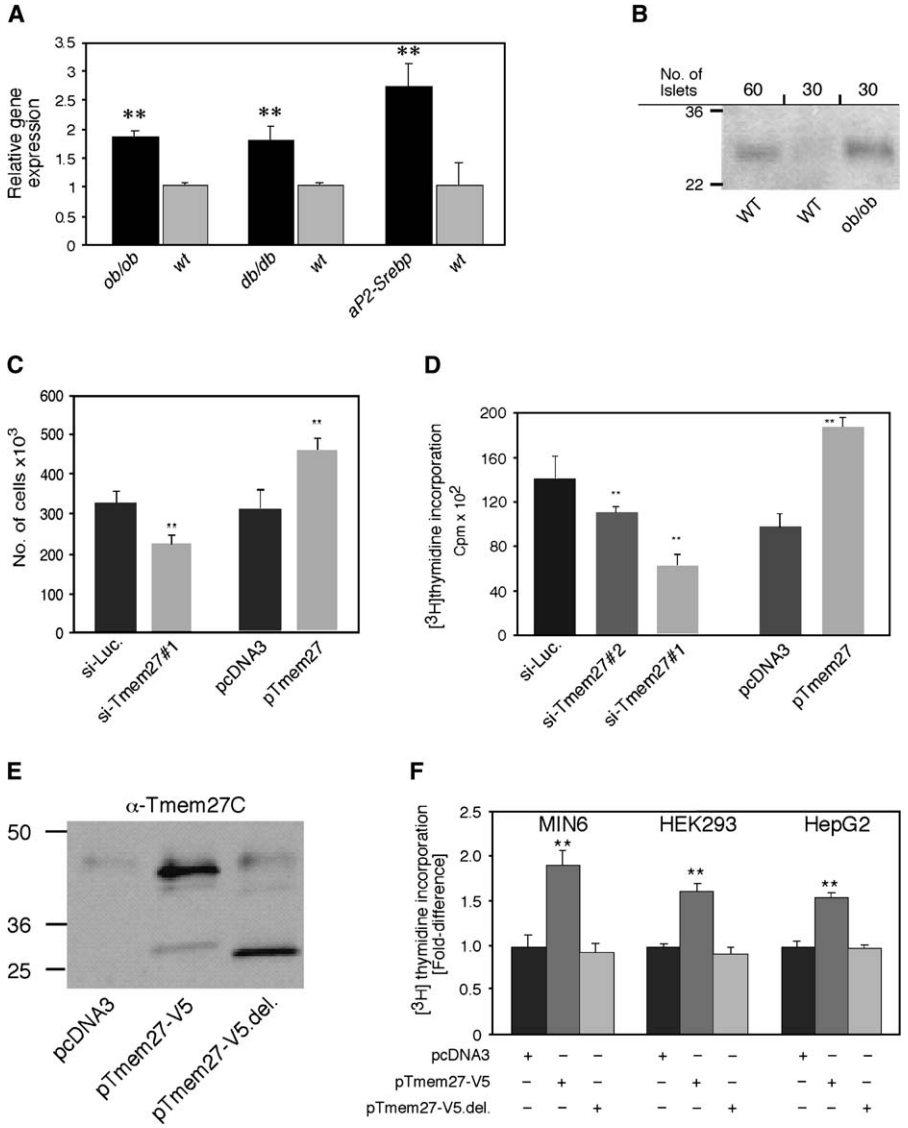

Figure 6. Tmem27 increases β cell replication in vitro

A) Tmem27 expression levels were measured in islets isolated from *ob/ob*, *db/db*, *aP-Srebp-1c* and wild-type littermate control mice with quantitative RT-PCR. Tmem27 expression was evaluated relative to β-actin levels in the same sample. $^{**}p < 0.01$.

B) Isolated islets from wild-type and *ob/ob* mice were matched for number and size and incubated in equal volumes of media for 72 hr. Soluble protein was detected with anti-Tmem27N.

C) MIN6 cells were electroporated with siRNAs targeting luciferase or Tmem27 and pcDNA3 or pTmem27. Cells were trypsinized 48 hr after electroporation, stained with trypan blue and counted with a hemocytometer. Each value represents a mean of six independent experiments. $^{**}p < 0.01$.

D) MIN6 cells were electroporated as denoted and cell replication was measured by [^{3}H]thymidine incorporation. $^{**}p < 0.01$.

E) MIN6 cells were electroporated with pcDNA3, pTmem27-V5, or pTmem27-V5del., which lacks amino acid residues 17-129. The deletion mutant is expressed as a ~30 kDa protein.

F) MIN6, HepG2 and HEK293 cells were transfected with pcDNA3, pTmem27-V5 or pTmem27-V5.del. Cell replication was measured by [^{3}H]thymidine incorporation. $^{**}p < 0.01$.

compared to wild-type littermates. Tmem27 is essential for optimal β cell growth in vitro and transgenic mice overexpressing Tmem27 exhibit increased islet mass. Promoter analysis and chromatin immunoprecipitation demonstrate that Tcf-1 binds to conserved TCF1 binding sites in the Tmem27 promoter and that it activates transcription of this gene.

Tmem27 is a homolog of angiotensin-converting enzyme-related carboxypeptidase (ACE2) and has previously been localized to the luminal surface and cytoplasm of collecting ducts (Zhang et al., 2001; Turner and Hooper, 2002). During the development of mouse kidney, Tmem27 is detectable at day 13 of gestation in the ureteric bud branches. Its expression is progressively increased during later stages of the gestation extending into the neonatal periods and then is decreased in adult life (Zhang et al., 2001). Interestingly, we found normal levels of Tmem27 mRNA in the kidneys of *Tcf1*$^{-/-}$ animals (data not shown). Tcf1 expression in adult kidneys is restricted to the proximal and distal tubules, whereas Tcf2, a related protein that can form heterodimers with Tcf1 and shares 93%, 75% and 47% sequence identity in their DNA binding domains, dimerization domains, carboxyl-terminal activation domains, respectively, is mainly localized in the collecting ducts (Rey-Campos et al., 1991; Coffinier et al., 1999). Tmem27 is specifically expressed in the collecting tubules and therefore overlaps in its expression with Tcf2, indicating that Tcf2 homodimers may regulate the expression of Tmem27 in these cells in the adult kidney. In pancreatic islets of *Tcf1*$^{-/-}$ mice, Tmem27 expression is profoundly reduced, indicating that Tcf2 cannot substitute for Tcf1. This may be explained by different DNA binding specificities and/or by the higher Tcf1 expression levels compared to Tcf2 in pancreatic islets.

We found that Tmem27 is expressed at the earliest stages of pancreatic development (E10.5). Tmem27 is expressed in hormone-positive cells throughout development but becomes restricted to pancreatic β cells in the postnatal period. We did not detect Tmem27 expression in Ngn3-positive neuroendocrine precursor cells (data not shown). This expression pattern is reminiscent of the temporal and spacial expression of Pdx-1, an essential transcription factor for pancreas development, differentiation and insulin gene transcription (Jonsson et al., 1994; Offield et al., 1996; Ahlgren et al., 1998). Indeed, we have identified a conserved binding site of Pdx-1 in the Tmem27 promoter

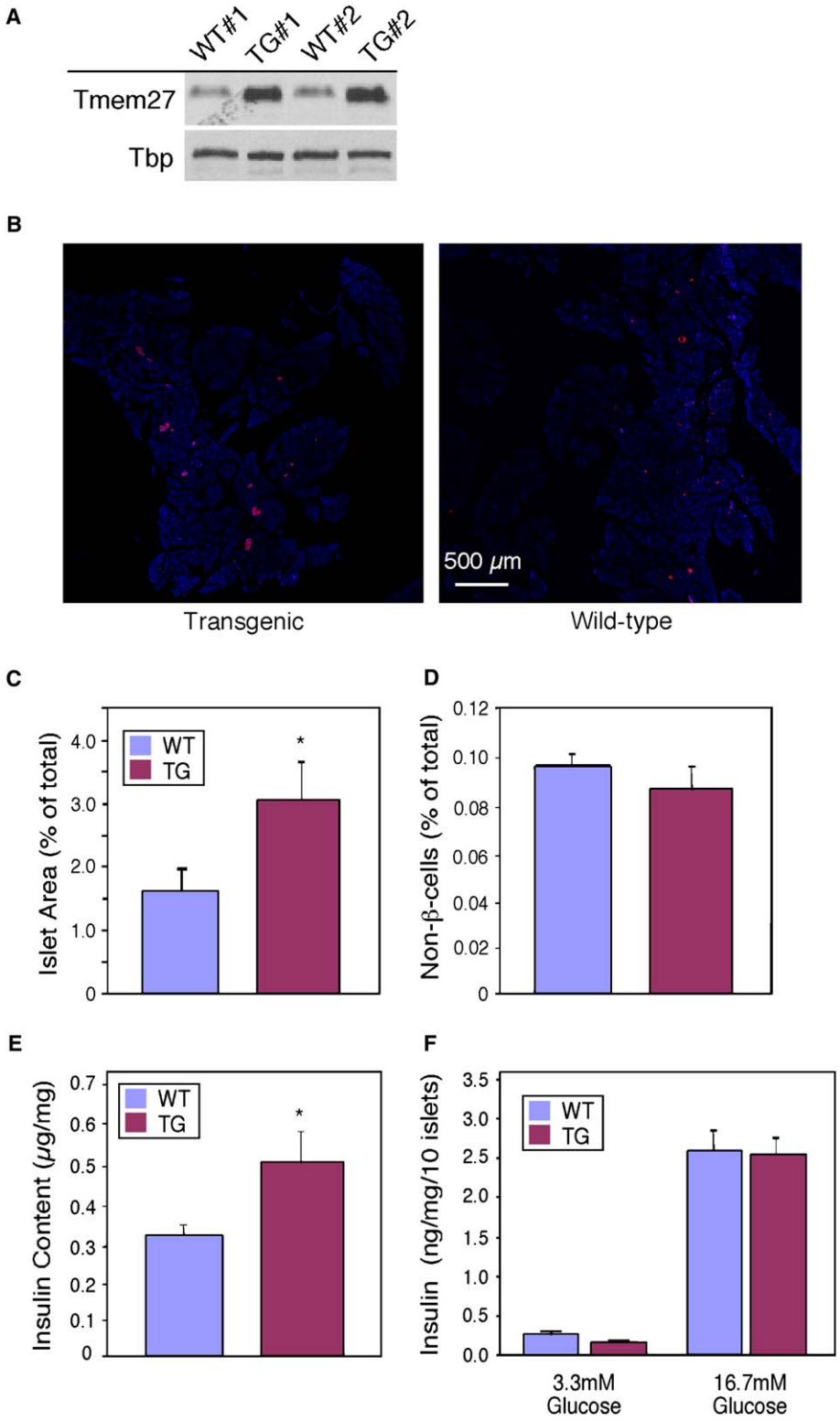

Figure 7. Increased expression of Tmem27 in pancreatic β cells leads to increased islet mass

A) Increased expression of Tmem27 was detected with anti-Tmem27C in Western blots of islets isolated from RIP-Tmem27 transgenic mice and wild-type littermate controls.

B) Immunohistochemistry of whole pancreata from transgenic and control littermate mice (n = 3). Cross-sections were embedded in paraffin and stained for insulin using anti-insulin antibodies. Images are representative of each genotype at 5x magnification.

C) Insulin staining in 7 μm sections was quantified using Metamorph software. At least 50 islets were quantified for each pancreas in sections greater than 200 μm apart. *$p < 0.05$.

D) Quantification of non-β cells of islets was performed by immunostaining with a cocktail consisting of anti-glucagon, somatostatin and pancreatic polypeptide antibodies. Analysis was carried out as in (**C**).

E) Whole pancreata from transgenic and wild-type mice (n = 5) were isolated and homogenized in acid/ethanol. Insulin content was normalized per pancreas weight. *$p < 0.05$.

F) Insulin secretion of size-matched islets of transgenic mice and wild-type littermates in response to glucose.

that partially overlaps with the Hnf1 site and which exhibits binding activity in EMSA analysis (Figures 1B and 1D), suggesting that Pdx-1 may also be a critical regulator of Tmem27. These data make it tempting to speculate that the membrane–bound or soluble form of Tmem27 contributes to the defect observed in Pdx-1 deficient mice, possibly by acting as a receptor or a signaling molecule (Johnson et al., 2003).

We found that the N-terminal, extracellular domain of Tmem27 is cleaved and released from the plasma membrane of pancreatic β cells. Tmem27 does not colocalize with insulin granules or synaptic-like microvesicles, thereby ruling out the possibility that Tmem27 is released by the regulated secretory pathway. This is further supported by the observation that the cleaved protein cannot be detected in whole-cell extracts of

MIN6 cells and that release of the cleaved form of Tmem27 is not regulated by glucose. Interestingly, cleavage of Tmem27 only occurs in pancreatic β cells and could not be detected in cells that were transfected with a Tmem27 expression vector. This may suggest that Tmem27 is cleaved by a β cell-specific or -enriched protease. Receptor shedding has been reported for members of diverse families of transmembrane receptors. For instance, the precursor form of hepatocyte growth factor is associated with the cell surface and biological function is dependent on proteolytic cleavage of an extracellular domain by the serine protease hepatocyte growth factor activator (HGFA)(Naldini et al., 1992; Miyazawa et al., 1993). Other receptors can bind to ligands upon cleavage and inhibit their activity. One example is the growth hormone binding protein (GHBP), which derives from proteolytic shedding of the GH receptor (GHR) extracellular domain and is complexed to a substantial fraction of circulating GH (Wang et al., 2002). Proteolytic shedding of receptors may not just release ligands or ligand binding proteins but can also be a means to regulate receptor function. For instance, one of the mechanisms that has evolved to modulate TNF function is the proteolytic cleavage of its cell surface receptors (Xanthoulea et al., 2004). The biological relevance is highlighted by identifications of mutations affecting shedding of the p55TNF receptor that have been linked with the development of the TNFR-associated periodic syndromes (McDermott, 2001). Our studies support a model by which the full-length, membrane-bound form of Tmem27 is responsible for stimulating cell replication: i. Overexpression of full-length Tmem27 in β cell lines and non-β cells that do not cleave Tmem27 leads to increased cell replication, ii. Overexpression of a truncated form in β cells and non-β cells has no effect on cell replication, and iii. Conditioned media or coculture experiments failed to provide evidence that the soluble form of Tmem27 stimulates cell replication. These studies indicate that identification of the cleavage enzyme that processes Tmem27 could be therapeutically used to develop drugs that inhibit the activity of this protease. Such an inhibitor may therefore reduce cleavage of Tmem27 and lead to constitutive receptor activation, thereby increasing β cell mass. The role of the extracellular, soluble form of Tmem27 is currently unknown and future studies need to establish if it serves as a ligand, a ligand binding protein or a receptor. However, its unique properties, including pancreatic β cell-specific and constitutive release, make it tempting to hypothesize that it may be exploited in the future as a biomarker for islet mass if sensitive RIAs or ELISAs can be developed to detect this protein in serum samples.

In this study we have also established that Tmem27 controls islet growth in vivo. The expression of Tmem27 is reduced in *Tcf-1*$^{-/-}$ mice and increased in three animal models of islet hypertrophy: *ob/ob*, *db/db* and *aP2-Srebp-1c* transgenic mice. It is interesting that expression of Tmem27 is also increased in the hypertrophic kidneys after renal ablation, indicating that it may play a role in compensatory growth responses to organ injury (Zhang et al., 2001). Significantly, two independent lines of transgenic mice with increased expression of Tmem27 in pancreatic β cells exhibited a ~2-fold increase in pancreatic islet mass and insulin content. Overexpression of Tmem27 in β cells had no effect on non-β cell mass, further supporting the notion that the full-length, membrane bound form is responsible for stimulating cell growth. Although under normal chow diet we did not observe alterations of glucose homeostasis, increased β cell mass together with unaltered glucose sensing will likely be beneficial in insulin-resistant states. Future studies with loss-of-function and gain-of-function mutations will further elucidate the role of Tmem27 in the maintenance of islet mass and insulin secretion. Such studies will validate Tmem27 or its inactivating protease as a novel pharmacological target for the treatment of diabetes.

Experimental procedures

Experimental animals

All animal models were housed in Laboratory of Animal Research Center (LARC), a pathogen-free animal facility at the Rockefeller University. The animals were maintained on a 12 hr light/dark cycle and fed a standard rodent chow. Genotyping of transgenic mice was performed on DNA isolated from 3 weeks old mice by PCR (Lee et al., 1998).

Vectors

The reporter plasmid pT27luc-wt was generated by cloning an 815 bp fragment of the mouse Tmem27 promoter into pGL2-luciferase. The reporter plasmids pT27luc-m1 and -m2 are identical to pT27luc-wt except for mutated TCF1 binding sites at positions −56 to –59 and –116 to –119. Vector pTmem27.V5 is generated by cloning a PCR fragment of 696 bp that encompasses 30 bp of 5′UTR of Tmem27 cDNA and the rest of the open reading frame except for the stop codon into pcDNA3.1/V5-His-TOPO vector from Invitrogen. Vector pTmem27-V5.del. was generated by deleting amino acid residues 17–129 of pTmem27.V5 vector using a PCR approach. The sequences of all constructs were confirmed by DNA sequencing.

Antibodies

Two peptides (anti-Tmem27N: VQSAIRKNRNRINSAFFLD and anti-Tmem27C: GIPCDPLDMKGGHINDGFLT) were synthesized and processed to >90% purity, conjugated to KLH and used for immunization of rabbits (Bethyl Laboratories, Texas). Antisera were affinity purified and tested by western blotting and immunohistochemistry. Affinity purified antisera were used for all studies. Other antibodies used for immunoblotting and immunohistochemistry were obtained from the following sources: anti-insulin (Linco), anti-glucagon (Linco), anti-V5 (Invitrogen), anti-Tcf1 (Active Motif), anti-HA (Covance), anti-Glut2 (R&D Systems), anti-synaptophysin (Chemicon), anti-somatostatin (Cell Marque), anti-PP (Linco), and anti-Pdx1 (gift from Chris Wright). Rhodamine red conjugated donkey anti-guinea pig (Jackson Labs), Alexa 488 donkey anti-rabbit (Molecular Probes).

Cell culture

MIN6 cells were cultured with DMEM medium containing 25 mM glucose, 15% fetal bovine serum, and 5.5 μM 2-mercaptoethanol. INS-1 cells were cultured with RPMI 1640 medium containing 11.1 mM glucose and 5% fetal bovine serum and 10 mM Hepes (pH 7.4). HepG2 cells were cultured with DMEM medium containing 25 mM glucose and 10% fetal bovine serum. Pancreatic islets were cultured in RPMI-1640 medium.

Transient transfections and luciferase assay

Fugene reagent (Roche) for HepG2 cells and Lipofectamine 2000 (Invitrogen) for MIN6 cells were used according to the manufacturer's directions in transient transfections. 0.5 μg of luciferase reporter construct, expression vector and CMV-LacZ were added per 35 mm dish. Luciferase was normalized for transfection efficiency by the corresponding β-galactosidase activity (Shih et al., 2001).

Crosslinking of proteins in cell lysates

MIN6 cells, grown to 90% confluency in 6 well plates, were harvested and resuspended in reaction buffer and reagent in 50 μl volume and incubated for 2 hr at 4ºC. Reactions were stopped by adding 50 mM Tris-HCl (pH 7.4) for 10 min on ice. Cells were then washed with PBS and lysed in RIPA buffer in the presence of protease inhibitors for 15 min at 4ºC. Cell lysates were centrifuged for 5 min at 10,000 × g and the supernatants were subjected to reducing and nonreducing SDS-PAGE followed by immunoblotting. Crosslinking reagents and buffers: BMH (Pierce) was dissolved in DMSO and incubated in PBS, and DTBP (Pierce) was dissolved in water and incubated in 0.2 M triethanolamine (pH 8.0).

Inhibition and enzymatic cleavage of N-glycosylation

MIN6 cells that express pV5-TMEM27 were incubated with indicated concentrations of tunicamycin (Sigma) dissolved in DMSO and with DMSO alone for 12 hr at 37ºC. Cell lysates were then subjected to SDS-PAGE and immunoblotting with anti-V5 antibody.

Intact N-linked glycans were removed from the soluble portion of TMEM27 with the recombinant enzyme N-glycanase (Prozyme, San Leandro, CA). Supernatants from MIN6 cells and pancreatic islets were denatured in 20 mM sodium phosphate (pH 7.5), 0.1% SDS, and 50 mM β-mercaptoethanol by heating at 100ºC for 5 min. NP-40 was added to a final concentration of 0.75% and reaction was incubated with N-glycanase for 3 hr at 37ºC.

Electrophoretic mobility shift assays

Electrophoretic mobility shift assays (EMSA) analysis was performed as described previously (Shih et al., 2001) with minor modifications. Assay was performed with 10 μg of whole-cell extracts in binding buffer (20 mM Hepes [pH 7.9], 10% glycerol, 150 mM NaCl, 1 mM DTT). Whole-cell extracts were incubated with ^{32}P-labeled double-stranded oligonucleotide probes containing the wild-type or mutant Tcf1 binding sites in the TMEM27 promoter (sequences: 5′-GGAGATTTTCGTAAATAACTGACA -3′, 5′-GGGCGTTAATT ATTAAACCTTTTA-3′ and 5′-GGGCAGAGATTATTAAACCTTTTA-3′, respectively). Cold competitor was an unlabeled double-stranded oligonucleotide containing the Tcf1 binding site in the Fxr-1 promoter (sequence: 5′−GAT GGGGGTTAATCAAGTAAACCACAC−3′). Supershifts were carried out with an anti-Tcf1 antibody (Geneka Biotechnology Inc., Montreal, Canada). ChIP analysis was carried out using isolated primary hepatocytes and isolated islets from *C57/B6* mice or MIN6 cells, and the ChIP Assay kit (Upstate Cell Signaling Solutions, Lake Placid, NY) according to the manufacturers protocol. Tcf1 was precipitated with anti-HNF-1α antibody and DNA was amplified using primers sequences: 5′-ACAGGAGGCAGGTGGGAGGCTT CT -3′ and 5′-CCCGGATTAGGGTATCGGAGAA -3′). Primers for apoM were 5′-GGGCTCAGCTTTCCTCCTA-3′ and 5′-CTCCGCCTTAACTGTTCTC TGATG -3′).

Whole-cell extract preparation

MIN6 cells were grown to 90% confluency in 150 mm tissue culture dishes. Cells were washed once in ice-cold PBS and scraped into 3 ml PBS. Cells were centrifuged at 4,000 × g for 4 min and resuspended in 2 volumes of high-salt extraction buffer (400 mM KCl, 20 mM Tris [pH 7.5], 20% glycerol, 2 mM DTT, 1x complete TM protease inhibitors (Boehringer Mannheim), and 20 μg/mL Aprotinin). Cell-lysis was performed by freezing and thawing, and the cellular debris was removed by centrifugation at 16,000 × g for 10 min at 4ºC.

Pulse-chase experiment with ^{35}S-labeled Tmem27

2 × 10^5 MIN6 cells were plated in 35 mm dishes and incubated in methionine-free DMEM (DMEM-Met) for 70 min at 37ºC. 200 μCi/mL of [^{35}S]methionine was added to DMEM-Met and cells were labeled in this media for 2 hr at 37ºC. At the end of the pulse period, MIN6 cells were chased with complete growth medium for different periods. At the indicated time points, supernatants were collected and cells were lysed for immunoprecipitation. Cells were washed in ice cold PBS five times and scraped into PBS and centrifuged for 5 min at 2000 rpm. Cells were suspended in lysis buffer (20 mM Tris-HCl [pH 7.4], 150 mM NaCl, 1% NP40, 1mM EDTA and protease inhibitors) and sonicated 5 s for 4 times. 0.25% sodium deoxycholate was added to the samples, which were then mixed and incubated on ice for 15 min. Samples were centrifuged for 15 min at max speed at 4ºC and the supernatant from the lysates were immuno-precipitated with α-Tmem27C for 16 hr at 4ºC followed by incubation with Protein G-Sepharose for 1 hr. Collected MIN6 supernatants were adjusted to 20 mM Tris-HCl (pH 7.4) and 1% NP40 along with protease inhibitors. α-Tmem27N antibodies were used to immunoprecipitate cleaved protein for 16 hr at 4ºC followed by incubation with Protein G-Sepharose for 1 hr. The sepharose beads were washed in ice-cold PBS 5-times for 5 min each and resuspended in SDS sample buffer (2% SDS, 62.5 mM Tris [pH 6.8]). Samples were boiled for 5 min and supernatants were run on 4%–15% gradient SDS gels. Gels were processed for autoradiography and exposed on film.

In vitro insulin secretion and hormone measurements

Mouse islets were isolated and incubated in different glucose concentrations after an overnight culture. Insulin and glucagon were extracted from pancreata with acid ethanol (10% glacial acetic acid in absolute ethanol), sonicated for 10 min, and centrifuged 2 times at 4ºC at 12,000 × *g* for 10 min. Supernatants were collected and stored at −20ºC for insulin and glucagon determinations by using sensitive RIA kits (Linco Research).

Pancreatic islet and RNA isolation

Pancreatic islets were isolated from 6 to 8 week-old mice. We used collagenase digestion and differential centrifugation through Ficoll gradients, with a modification of procedures previously described (Shih et al., 2002). Total RNA was then extracted using TRIzol reagent (Gibco-BRL) and following the manufacturer's instructions. Contaminating genomic DNA was removed using 1μl of RNase free DNase-I (Boehringer) per 5μg of RNA.

Islet morphometry

The pancreata were fixed in paraformaldehyde and stained for insulin and pool of glucagon, pancreatic polypeptide and somatostatin as described above. Sections (7μm) through the entire pancreas were taken, and every sixth section was used for morphometric analysis. At least 288 nonoverlapping images (pixel size 0.88μm) were scanned using a confocal laser-scanning microscope (Zeiss LSM 510, Germany). The parameters measured in this study were analyzed using integrated morphometry analysis tool in the Metamorph Software Package (Universal Imaging Corporation, PA). The area covered by cells stained by insulin or non-β cell pool was integrated using stained objects that are greater than 10 pixel in size.

RT-PCR

Total RNA was extracted using TRIZOL reagent (Invitrogen) and 10 μg of RNA was treated with 5U of RNase-free DNase-I (Ambion). cDNA was synthesized using Moloney leukemia virus reverse transcriptase with dNTPs and random hexamer primers (Invitrogen). The cDNAs provided templates for PCRs using specific primers in the presence of [α-^{32}P]dCTP and Taq polymerase as previously described (Shih et al., 2001). Quantitative PCR was performed using the Sequence Detection System 7700 (Applied Biosystems) for amplification and specific sequence detection. Forward and reverse PCR primers were used at a final concentration of 300 nM, and probes, containing a 5′ fluorophor (6-FAM) and a 3′ quencher (TAMRA), were used at a final concentration of 100 nM. Expression of Tmem27 was evaluated relative to the mRNA expression of the housekeeping gene β-actin in the same sample. Cycling parameters were: 2 min, 50ºC; 10 min, 95ºC; and 40 times: 30 s, 95ºC; 1 min, 60ºC. Primers and probes were purchased from Applied Biosystems.

Immunoblotting and immunohistochemistry

Cytosolic protein extracts were separated by SDS-PAGE (4%–15%) and transferred onto a nitrocellulose membrane (Schleicher & Schuell) by electroblotting. TMEM27 was detected with anti-Tmem27N and anti-Tmem27C antisera (1:500). Membranes were incubated with primary antibodies overnight at 4ºC. Incubations containing the secondary antibody were performed at RT for 1 hr. SDS-PAGE under nonreducing conditions was performed under conditions omitting DTT from the sample buffer.

MIN6 cells were plated on coated slides (Nalge Nunc Int.) and fixed with 4% paraformaldehyde at 4ºC for 20 min. Mouse islets were dissociated for 5 min at 37ºC in the presence of 0.01% Trypsin-EDTA and were plated in collagen coated slides and fixed the same way. Slides were incubated in 0.01% saponin with 3% normal donkey serum in PBS for 30 min at room temperature and anti-Tmem27N and anti-Tmem27C (1:20) were added overnight at 4ºC along with anti-insulin (1:600), anti-Glut2 (1:50), and anti-synaptophysin (1:500). Secondary antibodies were added for 30 min at RT.

Pancreata were fixed in 4% paraformaldehyde at 4ºC for 4 hr and embedded in paraffin. 7 μm sections were cut and after deparaffinization, antigen-unmasking was performed by microwaving slides in 0.01 M sodium citrate (pH 6.0). Sections were permeabilized in 0.1% Triton-X-100 and incubated in 3% normal donkey serum in PBS for 30 min. Staining was completed as above.

Electron microscopy studies

MIN6 cells were fixed in 4% paraformaldehyde and 0.02% glutaraldehyde in 0.1 M cacodylate buffer (pH 7.4) for 2 hr. The cells were washed with PBS and embedded in 10% gelatin and refixed as above. Cell pellets were cryoprotected using a 2.3M sucrose solution in PBS, and samples were stored in liquid nitrogen until use (Griffiths et al., 1983). Cryo, ultrathin sections were

cut using glass knives in a Reichert-Jung FC-4E cryo-ultramicrotome. The sections were collected on Formvar-carbon coated nickel grids, blocked with 1% BSA-PBS and incubated with anti-Tmem27C at a 1:10 dilution. Incubation was stopped by washing 2 times with PBS, 15 min each. The sections were then incubated with goat anti-rabbit IgG conjugated to 10 nm gold particles (Amersham Life Science, Arlington Heights, IL). The grids were processed and stained as desribed previously (Tokuyasu, 1973).

Thymidine incorporation studies

[^{3}H]Thymidine incorporation in 5×10^4 cells/well in 24-well culture plates was assayed as follows. 48 hr after electroporation, cells were incubated in growth arrest medium (0.5% FCS) for the next 24 hr and then incubated for an additional 24 hr in normal growth medium. For the last 4 hr of the incubation, 0.25 μCi/well [^{3}H]methylthymidine (Perkin Elmer) was added. After completion, cells were rinsed twice in ice-cold PBS, and incubated with 10% trichloroacetic acid (TCA) on ice for 20 min. After washing with 10% TCA, cells were solubilized in 0.2M NaOH/1% SDS for 10 min at room temperature. TCA-insoluble materials were neutralized with 0.2M HCl, and radioactivity was determined by a liquid scintillation counter.

RNA interference

Synthetic siRNAs were synthesized by Dharmacon Research (Lafayette, CO). siRNAs were designed for mouse TMEM27 (NM_020626) and Luciferase. The target sequences of siRNAs are: siTMEM27#1: gaagtacagtcggccataa, siTMEM27#2: ctacctatgctgatttaat. 3μg of each siRNA per 1×10^6 cells were electroporated into MIN6 cells.

Statistical analysis

Results are given as mean ± SD. Statistical analyses were performed by using a Student's t test, and the null hypothesis was rejected at the 0.05 level.

Supplemental data

Supplemental Data include Supplemental Experimental Procedures and can be found with this article online at http://www.cellmetabolism.org/cgi/content/full/2/6/385/DC1/.

Acknowledgments

We thank A. Viale for help and providing technical expertise in gene expression analysis. This work was supported by a grant from the Juvenile Diabetes Research Foundation and an unrestricted grant from Bristol-Myers Squibb (Metabolism) and the Deutsche Forschungsgemeinschaft (DFG).

Received: May 20, 2005
Revised: September 25, 2005
Accepted: November 3, 2005
Published: December 6, 2005

References

Accili, D. (2001). A kinase in the life of the β cell. J. Clin. Invest. *108*, 1575–1576.

Ahlgren, U., Jonsson, J., Jonsson, L., Simu, K., and Edlund, H. (1998). beta-cell-specific inactivation of the mouse Ipf1/Pdx1 gene results in loss of the beta-cell phenotype and maturity onset diabetes. Genes Dev. *12*, 1763–1768.

Bock, T., Pakkenberg, B., and Buschard, K. (2003). Increased islet volume but unchanged islet number in ob/ob mice. Diabetes *52*, 1716–1722.

Bonner-Weir, S. (2000a). Islet growth and development in the adult. J. Mol. Endocrinol. *24*, 297–302.

Bonner-Weir, S. (2000b). Perspective: Postnatal pancreatic beta cell growth. Endocrinology *141*, 1926–1929.

Bruning, J.C., Winnay, J., Cheatham, B., and Kahn, C.R. (1997). Differential signaling by insulin receptor substrate 1 (IRS-1) and IRS-2 in IRS-1-deficient cells. Mol. Cell. Biol. *17*, 1513–1521.

Butler, A.E., Janson, J., Bonner-Weir, S., Ritzel, R., Rizza, R.A., and Butler, P.C. (2003). Beta-cell deficit and increased beta-cell apoptosis in humans with type 2 diabetes. Diabetes *52*, 102–110.

Coffinier, C., Barra, J., Babinet, C., and Yaniv, M. (1999). Expression of the vHNF1/HNF1beta homeoprotein gene during mouse organogenesis. Mech. Dev. *89*, 211–213.

Dor, Y., Brown, J., Martinez, O.I., and Melton, D.A. (2004). Adult pancreatic beta-cells are formed by self-duplication rather than stem-cell differentiation. Nature *429*, 41–46.

Edlund, H. (2002). Pancreatic organogenesis—developmental mechanisms and implications for therapy. Nat. Rev. Genet. *3*, 524–532.

Finegood, D.T., Scaglia, L., and Bonner-Weir, S. (1995). Dynamics of beta-cell mass in the growing rat pancreas. Estimation with a simple mathematical model. Diabetes *44*, 249–256.

Flier, S.N., Kulkarni, R.N., and Kahn, C.R. (2001). Evidence for a circulating islet cell growth factor in insulin-resistant states. Proc. Natl. Acad. Sci. USA *98*, 7475–7480.

Geisler, N., Schunemann, J., and Weber, K. (1992). Chemical cross-linking indicates a staggered and antiparallel protofilament of desmin intermediate filaments and characterizes one higher-level complex between protofilaments. Eur. J. Biochem. *206*, 841–852.

Gradwohl, G., Dierich, A., LeMeur, M., and Guillemot, F. (2000). Neurogenin3 is required for the development of the four endocrine cell lineages of the pancreas. Proc. Natl. Acad. Sci. USA *97*, 1607–1611.

Griffiths, G.K., Simmons, C., Warren, K., and Tokuyasu, K.T. (1983). Immunoelectron microscopy using thin frozen sections: applications to studies of the intracellular transport of semliki forest virus spike glycoproteins. Methods Enzymol. *96*, 466–485.

Gu, G., Dubauskaite, J., and Melton, D.A. (2002). Direct evidence for the pancreatic lineage: NGN3+ cells are islet progenitors and are distinct from duct progenitors. Development *129*, 2447–2457.

Hagenfeldt-Johansson, K.A., Herrera, P.L., Wang, H., Gjinovci, A., Ishihara, H., and Wollheim, C.B. (2001). Beta-cell-targeted expression of a dominant-negative hepatocyte nuclear factor-1 alpha induces a maturity-onset diabetes of the young (MODY)3-like phenotype in transgenic mice. Endocrinology *142*, 5311–5320.

Jonsson, J., Carlsson, L., Edlund, T., and Edlund, H. (1994). Insulin-promoter-factor 1 is required for pancreas development in mice. Nature *371*, 606–609.

Johnson, J.D., Ahmed, N.T., Luciani, D.S., Han, Z., Tran, H., Fujita, J., Misler, S., Edlund, H., and Polonsky, K.S. (2003). Increased islet apoptosis in Pdx1+/− mice. J. Clin. Invest. *111*, 1147–1160.

Kahn, C.R. (2003). Knockout mice challenge our concepts of glucose homeostasis and the pathogenesis of diabetes. Exp. Diabesity Res. *4*, 169–182.

Kulkarni, R.N., Bruning, J.C., Winnay, J.N., Postic, C., Magnuson, M.A., and Kahn, C.R. (2002). Tissue-specific knockout of the insulin receptor in pancreatic beta cells creates an insulin secretory defect similar to that in type 2 diabetes. Cell *96*, 329–339.

Kulkarni, R.N., Otani, K., Baldwin, A.C., Krutzfeldt, J., Ueki, K., Stoffel, M., Kahn, C.R., and Polonsky, K.S. (2004). Reduced beta-cell mass and altered glucose sensing impair insulin-secretory function in betaIRKO mice. Am. J. Physiol. Endocrinol. Metab. *286*, E41–E49.

Lee, Y.H., Sauer, B., and Gonzalez, F.J. (1998). Laron dwarfism and non-insulin-dependent diabetes mellitus in the Hnf-1alpha knockout mouse. Mol. Cell. Biol. *18*, 3059–3068.

Lingohr, M.K., Buettner, R., and Rhodes, C.J. (2002). Pancreatic beta-cell growth and survival-a role in obesity-linked type 2 diabetes? Trends Mol. Med. *8*, 375–384.

McDermott, M.F. (2001). TNF and TNFR biology in health and disease. Cell. Mol. Biol. *47*, 619–635.

Miyazawa, K., Shimomura, T., Kitamura, A., Kondo, J., Morimoto, Y., and Kitamura, N. (1993). Molecular cloning and sequence analysis of the cDNA for a human serine protease reponsible for activation of hepatocyte growth factor. Structural similarity of the protease precursor to blood coagulation factor XII. J. Biol. Chem. *268*, 10024–10028.

Naldini, L., Tamagnone, L., Vigna, E., Sachs, M., Hartmann, G., Birchmeier, W., Daikuhara, Y., Tsubouchi, H., Blasi, F., and Comoglio, P.M. (1992). Extracellular proteolytic cleavage by urokinase is required for activation of hepatocyte growth factor/scatter factor. EMBO J. *11*, 4825–4833.

Offield, M.F., Jetton, T.L., Labosky, P.A., Ray, M., Stein, R.W., Magnuson, M.A., Hogan, B.L., and Wright, C.V. (1996). PDX-1 is required for pancreatic outgrowth and differentiation of the rostral duodenum. Development *122*, 983–995.

Parsons, J.A., Bartke, A., and Sorenson, R.L. (1995). Number and size of islets of Langerhans in pregnant, human growth hormone-expressing transgenic, and pituitary dwarf mice: effect of lactogenic hormones. Endocrinology *136*, 2013–2021.

Partis, M.D., Griffiths, D.G., Roberts, G.C., and Beechey, R.B. (1983). Cross-linking of multi sub-unit enzymes and immobilization of enzymes on solid supports. J. Protein Chem. *2*, 263.

Rey-Campos, J., Chouard, T., Yaniv, M., and Cereghini, S. (1991). vHNF1 is a homeoprotein that activates transcription and forms heterodimers with HNF1. EMBO J. *10*, 1445–1457.

Richter, S., Shih, D.Q., Pearson, E.R., Wolfrum, C., Fajans, S.S., Hattersley, A.T., and Stoffel, M. (2003). Regulation of apolipoprotein M gene expression by MODY3 gene hepatocyte nuclear factor-1alpha: haploinsufficiency is associated with reduced serum apolipoprotein M levels. Diabetes *52*, 2989–2995.

Scaglia, L., Smith, F.E., and Bonner-Weir, S. (1995). Apoptosis contributes to the involution of beta cell mass in the post partum rat pancreas. Endocrinology *136*, 5461–5468.

Shih, D.Q., Bussen, M., Sehayek, E., Ananthanarayanan, M., Shneider, B.L., Suchy, F.J., Shefer, S., Bollileni, J.S., Gonzalez, F.J., Breslow, J.L., and Stoffel, M. (2001). Hepatocyte nuclear factor-1alpha is an essential regulator of bile acid and plasma cholesterol metabolism. Nat. Genet. *27*, 375–382.

Shih, D.Q., Heimesaat, M., Kuwajima, S., Stein, R., Wright, C.V., and Stoffel, M. (2002). Profound defects in pancreatic beta-cell function in mice with combined heterozygous mutations in Pdx-1, Hnf-1alpha, and Hnf-3beta. Proc. Natl. Acad. Sci. USA *99*, 3818–3823.

Shih, D.Q., and Stoffel, M. (2002). Molecular etiologies of MODY and other early-onset forms of diabetes. Curr. Diab. Rep. *2*, 125–134.

Shimomura, I., Hammer, R.E., Richardson, J.A., Ikemoto, S., Bashmakov, Y., Goldstein, J.L., and Brown, M.S. (1998). Insulin resistance and diabetes mellitus in transgenic mice expressing nuclear SREBP-1c in adipose tissue: model for congenital generalized lipodystrophy. Genes Dev. *12*, 3182–3194.

Sorenson, R.L., and Brelje, T.C. (1997). Adaptation of islets of Langerhans to pregnancy: beta-cell growth, enhanced insulin secretion and the role of lactogenic hormones. Horm. Metab. Res. *29*, 301–307.

Svenstrup, K., Skau, M., Pakkenberg, B., Buschard, K., and Bock, T. (2002). Postnatal development of beta-cells in rats. Proposed explanatory model. APMIS *110*, 372–378.

Tokuyasu, K.T. (1973). A technique for ultracryotomy of cell suspension and tissue. J. Cell Biol. *57*, 551–565.

Tomita, T., Doull, V., Pollock, H.G., and Krizsan, D. (1992). Pancreatic islets of obese hyperglycemic mice (ob/ob). Pancreas *7*, 367–375.

Topp, B.G., McArthur, M.D., and Finegood, D.T. (2004). Metabolic adaptations to chronic glucose infusion in rats. Diabetologia *47*, 1602–1610.

Turner, A.J., and Hooper, N.M. (2002). The angiotensin-converting enzyme gene family: genomics and pharmacology. Trends Pharmacol. Sci. *23*, 177–183.

Waechter, C.J., and Lennarz, W.J. (1976). The role of polyprenol-linked sugars in glycoprotein synthesis. Annu. Rev. Biochem. *45*, 95–112.

Wiedenmann, B., Rehm, H., Knierim, M., and Becker, C.M. (1988). Fractionation of synaptophysin- containing vesicles from rat brain and cultured PC12 pheochromocytoma cells. FEBS Lett. *240*, 71–77.

Wilson, M.E., Scheel, D., and German, M.S. (2003). Gene expression cascades in pancreatic development. Mech. Dev. *120*, 65–80.

Withers, D.J., Gutierrez, J.S., Towery, H., Burks, D.J., Ren, J.M., Previs, S., Zhang, Y., Bernal, D., Pons, S., Shulman, G.I., et al. (1998). Disruption of IRS-2 causes type 2 diabetes in mice. Nature *391*, 900–904.

Wang, X., He, K., Gerhart, M., Huang, Y., Jiang, J., Paxton, R.J., Yang, S., Lu, C., Menon, R., Black, K., et al. (2002). Metalloprotease-mediated GH Receptor Proteolysis and GHBP Shedding. J. Biol. Chem. *277*, 50510–50519.

Yamagata, K., Nammo, T., Moriwaki, M., Ihara, A., Iizuka, K., Yang, Q., Satoh, T., Li, M., Uenaka, R., Okita, K., et al. (2002). Overexpression of dominant-negative mutant hepatocyte nuclear fctor-1 alpha in pancreatic beta-cells causes abnormal islet architecture with decreased expression of E-cadherin, reduced beta-cell proliferation, and diabetes. Diabetes *51*, 114–123.

Xanthoulea, S., Pasparakis, M., Kousteni, S., Brakebusch, C., Wallach, D., Bauer, J., Lassmann, H., and Kollias, G. (2004). Tumor necrosis factor (TNF) receptor shedding controls thresholds of innate immune activation that balance opposing TNF functions in infectious and inflammatory diseases. J. Exp. Med. *200*, 367–376.

Zhang, H., Wada, J., Hida, K., Tsuchiyama, Y., Hiragushi, K., Shikata, K., Wang, H., Lin, S., Kanwar, Y.S., and Makino, H. (2001). Collectrin, a collecting duct-specific transmembrane glycoprotein, is a novel homolog of ACE2 and is developmentally regulated in embryonic kidneys. J. Biol. Chem. *276*, 17132–17139.

Accession Numbers

Gene expression data have been deposited at GEO-NCBI under accession number GSE3544.